Published in final edited form as:
*Langmuir*. 2011 October 4; 27(19): 12074–12081. doi:10.1021/la202622s.

# Lysozyme adsorption on polyethylene surfaces: why are long time simulations needed?

**Tao Wei**, **Marcelo A. Carignano**, and **Igal Szleifer***
Department of Biomedical Engineering and Chemistry of Life Processes Institute, Northwestern University, Evanston, IL 60208

## Abstract

The adsorption of lysozyme onto a polyethylene (PE) surface in an aqueous environment was investigated with molecular dynamics (MD) simulation. The adsorption can be divided into three processes: diffusion to the surface, dehydration induced by hydrophobic surface-protein interactions followed by denaturation. The dehydration process is very long and takes around 70ns. Structural deformations start soon after the protein reaches the surface and continue during the whole trajectory. The hydrophobic residues are slowly driven toward the surface, inducing changes in the protein's secondary structure. The protein secondary structural components near the surface are more disturbed than those farther away from the surface. The lysozyme is adsorbed with its long axis parallel to the surface and displays an anisotropic mobility on the surface probably due to the intrinsic structure of the PE surface. Our study demonstrates the need of long-time atomistic simulation in order to gain a complete understanding of the adsorption process.

## Introduction

Protein adsorption at solid-solution interfaces is important in the development of biocompatible materials[1] and various biotechnological processes related to biosensors[2] and protein chips.[3] Furthermore, its fundamental understanding is of primary importance in the study of the interactions between life systems and synthetic materials, as the first step in the foreign response is the adsorption of blood proteins to the foreign surface.[4] Upon adsorption, biomolecules may undergo both physical and chemical transformations, which lead to changes in biological properties and activities. Protein adsorption has been studied with a variety of experimental techniques including atomic force microscopy (AFM) measurements,[5] optical waveguide lightmode spectroscopy (OWLS),[6] surface plasmon resonance (SPR),[7] Fourier transform infrared attenuated total reflectance (FTIR/ATR),[8] circular dichroism (CD),[9] neutron reflection[10,11] and fluorescence spectrum.[12] The experiments aim to understand the amount of protein adsorbed, its kinetics, secondary structural evolution of the adsorbed proteins and the motions of active sites, among other properties.

The complexity of the process of protein adsorption arises from the ability of the adsorbing molecules to change their configurations upon interaction with the surface. Furthermore, the native structure of the protein is the result of the delicate interplay between electrostatic, van der Walls and hydrophobic interactions coupled to solvent effects. This delicate balance can be disturbed in the presence of a large interacting surface. It has been well established that proteins adsorbing on hydrophobic surfaces tend to unfold.[13] However, there is no clear understanding of how this process takes place. A very insightful approach to study the

igalsz@northwestern.edu.

dynamics of protein adsorption at the atomistic scale is through the use of molecular dynamics (MD) simulations. The main limitation though is that in order to keep atomistic detail, very long simulations are prohibitively expensive. However, a number of groups have used different strategies to learn about various aspects of the adsorption process that help in our current understanding. For example, there are simulations performed without explicit account for the solvent molecules,[14] which while simplifying the system do not enable the study of specific solvation effects. A different approach consists in the use of continuous implicit solvent combined with energy minimization on the protein/surface complex in order to determine the optimal orientations for adsorption. Then, full atomistic MD simulations with explicit water is performed using the structures determined in the minimization step.[15–19] This methodology is very useful to learn about certain aspects of the protein-surface interactions, but again is limited in providing an understanding of the role and time scale of water effects involved in the development of the surface-protein interactions.

The motivation of the present work is to further our fundamental understanding of protein adsorption. In particular, we want to test whether many of the assumptions that are required to formulate a complete theory of the adsorption process of many proteins from solution to a finite density on the surface are valid. The type of questions that we want to address includes: Are the proteins mobile when they adsorb on hydrophobic surfaces? What is the role of water molecules in mediating the protein-surface interactions? What are the relevant time scales in the adsorption process? These questions are important in a variety of model adsorption processes.[20–25] For example, the random sequential adsorption model[22] assumes that once the proteins reach the surface they are immobile. Even if the adsorption process is kinetically controlled, the ability of the proteins to diffuse on the surface implies that the surface proteins may be equilibrated among themselves, even if they are not in thermodynamic equilibrium with the proteins in the bulk. There are a variety of different adsorption models that have been very successful in describing experimental data, however it is not always clear that the approximations made in their derivation are valid for the adsorption process. It is also important to emphasize that any complete treatment of protein adsorption has to be made through a multiscale approach due to the large range of time and length scales that are involved in the process.

In this work we attempt to address some of the questions formulated in the previous paragraph by looking in great detail at the adsorption of a single protein to a hydrophobic surface with the explicit account of all the atoms, including those of the solvent, water. To this end, we ran extensive, unbiased MD simulations that provide a picture of the adsorption in which there are three well defined regimes. First, approach of the protein to the surface through bulk diffusion; second, a very long dehydration process in which the protein also starts to show conformational changes, followed by the third process in which large structural alterations of the adsorbed protein take place.

To understand the changes in the protein upon adsorption it is important to recall what the native structure of the protein of interest is in solution. The tertiary structure of hen egg lysozyme can be thought of as two domains:[26,27] the α-domain (residues 1–35 and 85–129 forming four α-helix and a short $3_{10}$-helix near the C terminal) and the β-domain (residues 36–84 forming a triple-stranded antiparallel β-sheet, a long loop and a $3_{10}$-helix). The α-domain contains a core of closely packed hydrophobic side-chains referred to as the hydrophobic pocket. The dynamics of these two domains controls the frequency of opening/closing of the active site cleft[28] and directly relates with enzyme activity. Clearly, we aim to understand whether the adsorption of the protein to an hydrophobic surface can maintain this structural dependent function.

The native structure of any protein is intrinsically related to the solvation of the molecule. Proteins are in general very well solvated with a surrounding layer of water that, typically, has a larger density than that of the bulk water.[29–31] This is important for the stability of the protein in solution as well as for the biological function. The presence of a surface changes the hydration of the protein. This surface induced change is a long process usually disregarded in MD simulations. We will show that this is a very important part of the adsorption process that seems to facilitate changes in the protein structure.

In the next section we review the MD methods that we use. In the results sections we present the results from a typical long trajectory leading to adsorption. This trajectory was selected from a series of 27 similar simulations that differ from each other in the initial orientation of the protein with respect to the surface. The analysis of the effect of orientation will be published elsewhere. We follow the adsorption process for 300 ns, which starts with the approach of the protein to the surface, followed by a relatively long dehydration process of the water molecules between the protein and the surface. We monitor protein deformation in terms of its average shape and the motion of the residues relative to the PE surface. We study the domain stability and time evolution of the tertiary and secondary structures and characterize the mobility of the protein on the surface. Finally, we present some concluding remarks.

## Methods

The MD simulations were performed with the Gromacs (version 4.0.7) simulation package.[32] The interactions in the system were described by the OPLS-AA force field, combined with the TIP4P water model. The resulting trajectories were analyzed with our own scripts. A typical run employed 88 cores (Intel Xeon 2.27GHz) and produced approximately 20 ns per day. The integration of the dynamic equations was done using the leapfrog algorithm, with a time step of 1 fs. The system was maintained at a temperature of 300 K by coupling to a Berendsen thermostat, with a time constant of 0.1 ps. A spherical cut-off at 1.2 nm was imposed for all interactions.

For the preparation of the system we used a crystal structure of lysozyme (1AKI) from the Protein Data Bank (http://www.ncbi.nlm.nih.gov/). The amino acids histidine (His), arginine (Arg), and lysine (Lys) were protonated, while glutamate (Glu) and aspartate (Asp) were deprotonated resulting in a net charge of +8e that corresponds to the experimental conditions at pH 7. The N and C termini were capped uncharged.

The PE surface was constructed by replicating the crystalline ethylene unit cell in the three Cartesian directions. The resulting PE slab consists of 9×5×24 units cells and was rotated in such a way that the (010) plane is facing the solution. The atoms forming the ethylene monomers near the edges of the periodic box on the *y* direction were covalently bonded with the atoms of their periodic images, mimicking infinitely long chains. The PE surface was initially soaked in TIP4P water, and the water molecules were relaxed with a short NVT simulation at 300 K. Next, the system of PE surface and water were relaxed under NPT conditions at a temperature of 300 K and a pressure of 1 bar during 10 ns. The PE layer relaxed to reach an equilibrium thickness of 2.5 nm. In the following step, the system was assembled with one lysozyme, leaving a gap of at least 0.9 nm between the PE surface and the protein, as shown in Figure 1. Any water molecule within 0.3 nm of the lysozyme was removed. The system was neutralized by adding 8 $Cl^-$ ions. The interaction between the simulation box and its periodic images along the *z*-direction was effectively removed by inserting a vacuum slab of 2.2 nm on the top of the water box. Water molecules were kept inside the box by inserting a restraining layer of repulsive Lennard-Jones artificial atoms at fixed positions ($z$=10 nm). These settings resulted in a water slab of 6.6 nm from the top of

the PE layer up to the restraining layer, sufficient to guarantee enough space for the protein to rotate inside the cell without being affected by the top restraining layer. The total dimensions of the simulation box after the system was relaxed are 6.565×6.119×11.3 $nm^3$. We verified that the density of the system in the region of pure water was 1 $g/cm^3$.

The simulations were started with relaxation runs. The water molecules were firstly relaxed with energy minimization and a short run of MD (50 ps) at 300 K, maintaining PE and lysozyme fixed. The second step was to relax the PE surface and water with a series of simulations of 800 ps, which were carried out using the annealing protocol starting at a temperature of 10 K and reaching 300 K in 10 steps. In this way, the whole system (protein and the surface) was hydrated without any perturbation of the protein structure. Finally, production runs were carried out in the NVT ensemble, at 300 K, using 1 fs time step.

## Results

The process of protein adsorption from solution can be separated into transport to the surface followed by adsorption proper. The fraction of proteins that will adsorb upon contact with the surface is known to depend on the orientation of the protein with respect to the surface.[33] In this work we concentrate our attention on a long trajectory in which the protein adsorbs. We are interested in analyzing how the protein changes both its hydration state and its conformation upon contact with the surface. Figure 2 shows the structure of the protein adsorbed on the surface with a few layers of water. Visual inspection shows that the number of water molecules between the hydrophobic surface and the protein is small and the structure of the protein is rather different than the native one shown in Figure 1 (the exact quantification of both effects is shown below). We will show that the process of dehydration is very long, around 70 ns, followed by the denaturation of the protein, which takes an even longer time.

The complete quantification of the adsorption process can be made in several different ways. Here we choose to start by looking at the distance of closest approach between the protein and the surface together with the orientation of the protein with respect to the surface. The orientation of the protein is defined as the angle (θ) between the largest eigenvector of the radius of gyration tensor, with the sign defined from the center of mass to the Trp128, and the plane of the surface. The radius of gyration tensor is defined by

$$R^2_{\gamma,\delta}=\frac{1}{M}\sum_{i=1}^{N} m_i(\gamma_i-\gamma_{cm})(\delta_i-\delta_{cm}),\quad \gamma,\delta=x,y,z \tag{1}$$

where the sum runs over all the atoms $i$, $M$ is the total mass, $m_i$ is the mass of atom $i$ and δ and γ represent the coordinates.

Figure 3A displays the distance between the protein and the surface as a function of time. This distance ($z_{ps}$) is defined as the $z$-component of the distance between the center of mass of the carbon atoms corresponding to the top PE layer and the protein's atom closest to the surface (smallest $z$-coordinate). At very short times there is a sharp decrease of the distance, see inset, which reflects the transport of the protein from the solution (middle of the simulation box) to the surface. This process is very fast, due to the small size of the simulated box, and it is followed by a very long process that takes around 80 ns. The orientation of the protein, shown in Figure 3B, shows initially fluctuations between −10° and 10° and stabilizes to a constant angle of around 10° for the next 70 ns. Then the protein relaxes to a parallel orientation with the surface from $t$=80 ns up to the end of the simulation, i.e. $t$=300 ns. The complete parallel orientation coincides with the time in which the distance

between the protein and the surface is zero. It is interesting to note from the inset of Figure 3A that, in that scale, the protein-surface distance is constant suggesting that the adsorption process is complete. Clearly, as the full scale shows, this is not the case. It is also worth to mention that the rotation of the protein during the first stages of adsorption resembles the finding of Kubiak and Mulheran,[34] who studied adsorption of lysozyme on a charged solid surface.

How can we understand what is this initial long time process within the first 100 ns of simulation? We can find the answer by looking at the water molecules solvating the protein (and the surface). To this end we use the proximal radial distribution function[31,35–37] $pG(r)$, to quantify the changes in solvation as the adsorption process takes place. This quantity measures the radial distribution function of the oxygen of the water molecules from the atom of the lysozyme that is closest to them. The distributions are shown in Figure 4 for three different times along the adsorption process. For 1.9 ns what we have is the native protein solvated in solution, i.e. before it feels the presence of the adsorbing surface. The proximal radial distribution shows a small peak at 0.2 nm representing the hydrogen bond between the oxygen of the water and the hydrogen atoms from the protein. The much larger peak, at around 0.3 nm, represents mostly the water molecules acting as hydrogen bond donors. The three distributions show almost identical shapes with only small quantitative differences, in particular in the second peak and for the shortest time. This difference demonstrates the overall change in the number of water molecules hydrating the protein at various times. The information provided by these profiles is not enough to obtain an understanding of the changes in solvation as the adsorption process takes place. A better description is given by slicing the protein in regions which depend on the distance between the protein atoms and the surface.

In Figure 5A we show the proximal distribution functions for the water by dividing the protein in three regions as marked in the cartoon. The profiles, showing the solvation at the end of the simulation when the protein is adsorbed, are rather different, in particular the one that corresponds to the protein region in direct contact with the surface. There is a large depletion of water molecules for 0.25 nm ≤ $r$ ≤ 0.7 nm as compared to the other two regions. To better quantify this effect we calculate the number of water molecules in the full first hydration layer of the protein. This quantity is related to the integral of the proximal distribution from $r$=0 to $r$=0.5 nm, weighted by the number of protein's surface atoms in the corresponding regions. The hydrating water molecules are shown as a function of time for the three different protein regions in Figure 5B. The region in contact with the surface shows a decrease of water molecules, with a sharp drop at short times ($t$ < 1.5 ns) and continuing up to $t$ ~ 150 ns and then it fluctuates. We will discuss these fluctuations below since they represent important conformational changes upon adsorption. Due to the elongated average shape of the protein (see Figure 8 below), the total area of the top region is larger than the total area of the middle region; therefore, the absolute number of hydrating water molecules is larger on top section than on the middle section. The middle region as well as the upper part of the protein show small changes in their hydration throughout the simulation. However, in the last 100 ns of the simulation the number of water molecules hydrating the upper (middle) region of the protein increases (decreases). As it will be discussed below these changes are associated with frequent conformational changes of the protein on the surface. The result to highlight from Figure 5 is that the number of water molecules solvating the protein region in contact with the surface decreases showing that the slow relaxation of the distance between the protein and the surface in the first 100 ns, see Figure 3, is due to the dehydration of the region between the protein and the surface.

To further understand the changes associated with the adsorption process we look at the total interaction between the protein and the surface and a structural parameter called asphericity. The latter quantity is defined as

$$A_s = \frac{\sum_{i>j=1}^{3}\left(R_i^2 - R_j^2\right)^2}{2\left(\sum_{i=1}^{3}(R_i^2)\right)^2} \quad (2)$$

where $R_i^2$ correspond to the principal components (eigenvalues) of the radius of gyration tensor, see Eq. (1). $A_s = 0$ for a sphere, 1 for a perfect rod and values in between represent ellipsoids with varying ratios of the different axis. Figure 6 shows the time evolution of the surface-protein interaction and the asphericity. There are interesting parallels in the times when there are significant changes in both the asphericity and the interactions, manifesting the coupling between conformational changes and the resulting energetics. Before we analyze these effects it is important to emphasize that there are many other relevant contributions to the energy of adsorption. However, they are hard to quantify due to the large fluctuations characteristic to the systems size studied here. For example, the fluctuations in the water-water interactions are larger than the overall changes in the protein-surface interactions. This is simply due to the very large number of water molecules in the simulations, see e.g. Figure S1 of the supplementary information. Keeping this limitation in mind we move now to analyze the results presented in Figure 6.

The protein-surface interactions are attractive at all time, except at the very beginning of the simulations where the protein does not see the surface and thus $E_{ps} \approx 0$. During the first ~ 70 ns the protein-surface energy decreases quite sharply. This is the same time scale in which the dehydration process takes place, see Figure 3. Interestingly, there is a plateau for about 100 ns in the energy followed by a series of changes in which the energy decreases and increases. The asphericity shows an increase in value during the dehydration process, followed by a sharp drop and a plateau, which is shorter in time than the plateau in energy. Actually, there is not a one to one correspondence between the energy and the asphericity however, large changes in both quantities seem to be strongly correlated. Once more we see that the presence of a plateau, in this case in the energy and the asphericity, do not represent equilibrium or steady state, due to the small perturbational nature of the important dehydration process.

To further understand the changes in structure associated with the adsorption process we monitor the distance between the center of mass of each amino acid and the surface at different times. This is shown in Figure 7 for the early stages of adsorption, 10 ns, the end of dehydration on the surface-protein region, 100 ns, and the final stages of the simulation, 300 ns. From these results we can identify the regions of the proteins that suffer the largest deformation upon adsorption. The results suggest that the main deformations occur in the α-domain of the protein. In particular, the second part of α-domain (amino acids 85–129) that contains the C-terminal shows a more significant rearrangement than the rest of the protein. The first part of α-domain (amino acids 1–35) displays a deformation that does not involve the N-terminal. Particularly the residues (15–28), (105–115) and (116–129) have large displacements toward the PE surface. The intermediate β-domain (amino acids 36–84) is less affected by the adsorption. Based on the final conformation in the simulation, we identify seven adsorption sites composed of a mixture of strong hydrophobic (Val, Phe and Leu) and hydrophilic amino-acid residues. These sites are defined as follow: Site 1 (1–4), site 2 (33–52), site 3 (67–69), site 4 (84–86), site 5 (108–112), site 6 (120–123) and site 7(128–129). The first four sites participate in the initial contact of the protein with the surface, and remain adsorbed during the rest of the simulation. At the end of dehydration,

*t*=100 ns, site 5 in the second part of the α-domain is attracted to the surface. There are significant changes in the conformation of the second part of the α-domain at the end of dehydration and sites 5 and 7, which contains the C terminal, reach the PE surface at *t*=100 ns. Site 6 is adsorbed only after 300 ns of simulation.

Residues (15–28) in the first part of α-domain also have significant displacements but do not reach the PE surface. Large displacements in the regions of (105–115) and (116–129) can be qualitatively attributed to the attraction induced between the hydrophobic surface and the hydrophobic residues (Ala107, Trp108, Val109, Ala110, Trp111, Val120, Ala122, Trp123, Ile124 and Leu129). The turn-over or large displacements of the region (15–28) corresponds to the hydrophobic residues (Gly16, Leu17, Gly22, Leu25, Gly26 and Trp28). Details of the motions in the α-domain in connection with the tertiary and secondary structures will be discussed below.

We monitor the lysozyme's tertiary structure in terms of a shape (asphericity, $A_s$) and size (the radius of gyration, $R_g$) parameter, as shown in Figure 6 and Figure S2 (in the supporting document), respectively. There is an important degree of correlation between the two quantities. During the first 30 ns of simulation $R_g$ remains close to the value corresponding to the protein in solution, i.e. $R_g$=1.44 nm. The profiles of $A_s$ and $R_g$ show a steady increase up to 75 ns followed by a sudden drop. Other important variations in $A_s$ and $R_g$ occur between *t*=166 ns and *t*=183 ns. These sharp changes correspond to significant structural rearrangements (displacements towards the surface) in the second part of α-domain before 100 ns. More changes occur in the same region during the following 200 ns, together with an approach to the surface of residues (15–28) of the first part of the α-domain.

It is worth noting that the hydrophobic pocket, which exists in the native form of the lysozyme and serves as the binding site of aromatic chromophores such as ecosein, consists of residues (Tyr20, Tyr23, Trp28, Met105, Trp108 and Trp111) that are compactly packed in the α-domain.[38,39] Some residues of this pocket, typically tryptophan (28, 108 and 111), undergo the most significant approach towards the PE surface. The hydrophobic pocket maintains its close packing during the transport to the surface and in the early stages of dehydration. Details of the evolution of the hydrophobic pocket are displayed in Figure 8. From 30 to 75 ns, the protein undergoes elongation ($\delta A_s$=0.09) and expansion ($\delta R_g$= 0.12 nm). At *t*=75 ns the pocket disassembles, the protein undergoes a contraction reflected by the changes in asphericity ($\delta A_s$=−0.05) and radius of gyration ($\delta R_g$=−0.06 nm). The Trp residues (108 and 111) are attached to the surface, and the residues (15–28), which contain another part of the hydrophobic pocket, move towards the surface without reaching it. The intensive motions in the area of residues (106–115) result in the development of adsorption site 5 clearly visible at *t*=100 ns.

After the dehydration stage is complete ($t \approx 100$ ns) the residues (112–125) slowly deform and move toward the PE surface, leading to a slow increase in $A_s$ and $R_g$. However, between *t*=166 ns and *t*=183 ns fast changes in the protein's structure involving precisely those residues occur. A decrease in $A_s$ is associated with the detachment of the residues (112–125) from the PE surface at *t*=166 ns. The subsequent increase in $A_s$ at *t*=183 ns is associated with the readsorption of the same residues to the surface. The fluctuations in shape persist displaying a slower relaxation of the protein. Toward the end of the simulation, the region involving residues (111–125) undergoes a rotation that leaves site 6 adsorbed to the PE surface at *t*=300 ns.

Lysozyme is rich in secondary structures (α-helix: 36–40%; β-sheet: 5–7 %; turn: 22–44 %).[26,40] We used the Kabsch and Sander method[41] to define the different secondary structural components indicated in Figure 9. NMR measurements have shown that the

secondary structures of lysozyme in solution are close to the crystalline one.[26] Five α-helix and two anti-parallel β-sheet are the features that appear more frequently among the 50 NMR structures in solution (see Figure S3(a) in the supporting document). The time evolution of secondary structure elements during the simulation is shown in Figure 9.

To facilitate the discussion we define 8 regions: α-helix A (Cys6-His15), α-helix B (Leu25-Ser36), α-helix C (Thr89-Ser100), α-helix D (Trp111-Arg114), and α-helix E (Val120-Trp123); β-sheet F (Thr43-Arg45), β-sheet G (Thr51-Tyr53) and β-sheet H (Ile58-Asn59) forming the triple-stranded antiparallel structure.

During the protein transport to the surface there is no significant changes in the secondary structure: D and E transform to two $3_{10}$-helices.

The surface-induced rearrangements of the secondary structures start occurring in conjunction with the dehydration process, $t > 10$ ns. α-helix region B, which is adjacent to the surface and around the adsorption site 2, is partially unwound to become a short $3_{10}$-helix and a turn. α-helix C (Thr89-Ser100) is only partially disturbed.

The main β-sheet region F adjacent to the surface (corresponding to the adsorption site 2) is completely denaturated for $t > 20$ ns. As discussed above, the hydrophobic residues of (105–129) undergo large motions and some of them are eventually attracted to the surface to form adsorption sites 5 to 7 during and after dehydration. The $3_{10}$-helix structure D changes to a bend at $t \approx 70$ ns. Instead, the $3_{10}$-helix structure E transforms back to α-helix before reducing to a bend at $t \approx 150$ ns. The β-sheets G and H show almost no change during the entire trajectory. It is interesting to note that two new β-sheet regions (18–20, 23–25), located away from the surface, develop around the sites where a β-bridge was originally present.

In general, the secondary structures in the α-domain unfold substantially, whereas most parts of the β-domain remain relatively unchanged within the length of the trajectory. The surface-induced unfolding in both domains of the lysozyme is similar to what is generally observed in the bulk solution environment: the β-domain has a lower folding rate; its relaxation time ($\tau \approx 350$ ns) is one order of magnitude longer than that of α-domain.[42–44] Our large-scale simulation results (0.3 μs) demonstrate a similar trend of recent experimental measurements, in which the α-helix are denaturated while the β-sheet content undergoes no perceptible change at very low surface coverage of hen egg lysozyme on a poly(tetrafluroethylene) surface.[40] Interestingly, recent simulations results based on the two steps methodology; namely, implicit solvent energy minimization followed by a short full atomistic MD, predicts a larger stability of the α-helix motifs than the β-sheets that decay in a very short time.[45] The active site is also affected by the deformation of the protein as it adsorbs. The extent of this deformation, as quantified by the RMSD of residues Glu35, Asp52, Trp62, Trp63 and Asp101, is larger for the adsorbed protein after 300 ns (0.564 nm) than in solution after 5 ns (0.335 nm). It is expected, however, that the RMSD in the adsorbed case will depend on the orientation on which the protein adsorb. It would be interesting to experimentally monitor the protein activity as it gets adsorbed. In this way, one could determine the timescale of functional denaturation.

It is generally believed that proteins that denaturate upon adsorption become immobilized on the surface. Our simulations show that the protein is highly mobile on the surface, however visual inspection of the trajectory shows that the surface mobility is anisotropic. To quantify this effect for the case of lysozyme on a hydrophobic crystalline surface, we calculated the diffusion coefficient of the protein after the water depletion is completed, i.e. for $t > 200$ ns. The bulk diffusion coefficient of lysozyme is reported to be $5.84 \times 10^{-6}$ $cm^2/s$.[46] The presence of the surface breaks the symmetry of the motion and therefore it is convenient to

report the diffusion coefficient in the three orthogonal directions *x*,*y*, *z* where the surface is within the *x*,*y* plane and the *z* direction is perpendicular to it. Clearly, there is no diffusion in the direction perpendicular to the surface, since the protein is adsorbed. In the plane of the surface the diffusion is highly anisotropic with values of $D_x$ = 0:029 × $10^{-6}$ $cm^2$/s while $D_y$ = 4:1 × $10^{-6}$ $cm^2$/s. The direction of high mobility corresponds to the "tracks" that the crystalline PE presents to the adsorbed protein, see Figure 1. There are two important conclusions to be drawn from these results. First, the proteins are highly mobile, with one of the diffusion coefficient components not very far from the bulk value, even though they are denaturated and strongly adsorbed on the surface. Second, the motion of the protein is largely in the direction of the polyethylene chains. The mobility on the surface has important consequence for the way bulk proteins adsorb and need to be included. The surface adsorbed proteins, even though they may not leave the surface, they have the possibility of laterally equilibrate and thus assuming that the adsorbed proteins have equal chemical potential, albeit different from the proteins in the bulk, may be a good approximation to treat adsorption processes from bulk solution.

## Conclusion

We carried out large-scale atomistic molecular dynamics simulations to study the adsorption of a model system consisting of a lysozyme interacting with a polyethylene surface in an aqueous environment. We monitored the structural deformation of the protein as it adsorbs to the surface, the corresponding dehydration process and the mobility of the adsorbed protein onto the hydrophobic surface. The adsorption process can be divided in three stages: transport to the surface, dehydration and deformation, after the protein is in full contact with the surface. The lysozyme preserves its tertiary and secondary structures during the transport to the surface. Then, the water molecules trapped between the lysozyme and the surface are removed during the dehydration stage that lasts approximately 70 ns. During this stage, the protein starts to undergo structural relaxation and deformations that involve the displacement of hydrophobic residues toward the surface. This deformation process continues until the end of the trajectory. It is not clear if there will be additional conformational changes should the trajectory be continued. One could argue, based on the longest simulations, that there may be cooperative processes that happen on millisecond time scales. However, the studies of those processes in surfaces is prohibitively expensive for the protein-surface-solvent system treated here, even with the most advanced computation resources.[47] The conformation of the lysozyme after 300 ns is with its long axis parallel to the surface, and it is elongated and expanded with respect to the native conformation, with a significant loss of α-helix content, but preserving most of the β-sheet features. Interestingly, the mobility of the protein on the surface follows the crystalline structure of the substrate inducing a preferential diffusion parallel to the polyethylene chains.

Our results suggest that very long simulations are needed to understand the adsorption process in full. Moreover, the use of time independent quantities for relatively long periods of time may not be a good measure for equilibration. At several times during the simulation it appears that the system behaves as if it were in equilibrium, for example when the energy does not change from 80ns to 160ns. However, the continuation of the trajectory revealed additional large changes on structure. The plateau like structures are the result of the small perturbative nature of the dehydration process, however the simulations show clearly that at the end of this process dramatic changes occur. The constant improvement of simulation methodologies and computer hardware will enable the study of larger simulations in the future. The important conclusions from these simulations are the long time scale and important role of dehydration, the constant denaturation and the large mobility of the proteins on the surface. These are all important building blocks for the proper description

and development of coarse-grained models and molecular theories for the understanding of the complex adsorption process involving many proteins that cannot be treated with atomistic detail.

## Supplementary Material

Refer to Web version on PubMed Central for supplementary material.

## Acknowledgments

This work was partially supported by funded the Materials Research Science and Engineering Center (MRSEC) at Northwestern University under NSF Grant No. DMR-0520513. IS acknowledges the support from NSF under Grant CBET-0828046 and the NIH grant No. EB005772. MAC acknowledges the support from NSF under Grant CHE-0957653.

## References

1. Messersmith PB. Science. 2008; 319:1767–1768. [PubMed: 18369126]
2. Lasseter TL, Clare BH, Abbott NL, Hamers RJ. J. Am. Chem. Soc. 2004; 126:10220–10221. [PubMed: 15315415]
3. Zhu H, Bilgin M, Bangham R, Hall D, Casamayor A, Bertone P, Lan N, Jansen R, Bidlingmaier S, Houfek T, Mitchell T, Miller P, Dean RA, Gerstein M, Snyder M. Science. 2001; 293:2101–2105. [PubMed: 11474067]
4. Ratner, BD.; Hoffman, AS.; Schoen, FJ.; Lemons, JE. Biomaterials Science: An Introduction to Materials in Medicine. San Diego: Elsevier Academic Press; 2004.
5. Kim DT, Blanch HW, Radke CJ. Langmuir. 2002; 18:5841–5850.
6. Statz AR, Barron AE, Messersmith PB. Soft Matter. 2008; 4:131–139. [PubMed: 21472038]
7. Li G, Xue H, Gao C, Zhang F, Jiang S. Macromolecules. 2010; 43:14–16. [PubMed: 20228890]
8. Wei T, Kaewtathip S, Shing K. J. Phys. Chem. C. 2009; 113:2053–2062.
9. Billsten P, Wahlgren M, Arnebrant T, McGuire J, Elwing H. J. Colloid Interf. Sci. 1995; 175:77–82.
10. Su TJ, Green RJ, Wang Y, Murphy EF, Lu JR, Ivkov R, Satija SK. Langmuir. 2000; 16:4999–5007.
11. Lu JR, Su TJ, Thirtle PN, Thomas RK, Rennie AR, Cubitt RJ. Colloid Interf. Sci. 1998; 206:212–223.
12. Benesch J, Hungerford G, Suhling K, Tregidgo C, Mano JF, Reis RL. J. Colloid Interf. Sci. 2007; 312:193–200.
13. Buijs J, Norde W, Lichtenbelt JWT. Langmuir. 1996; 12:1605–1613.
14. Ravichandran S, Madura JD, Talbot J. J. Phys. Chem. B. 2001; 105:3610–3613.
15. Sun Y, Welsh WJ, Latour RA. Langmuir. 2005; 21:5616–5626. [PubMed: 15924498]
16. Raffaini G, Ganazzoli F. Langmuir. 2004; 20:3371–3378. [PubMed: 15875871]
17. Zheng J, Li LY, Chen SF, Jiang SY. Langmuir. 2004; 20:8931–8938. [PubMed: 15379529]
18. Zheng J, Li L, Tsao H, Sheng Y, Chen S, Jiang S. Biophys. J. 2005; 89:158–166. [PubMed: 15863485]
19. Wei T, Mu S, Nakano A, Shing K. Comput. Phys. Commun. 2009; 180:669–674.
20. Satulovsky J, Carignano MA, Szleifer I. P. Natl. Acad. Sci. USA. 2000; 97:9037–9041.
21. Fang F, Szleifer I. P. Natl. Acad. Sci. USA. 2006; 103:5769–5774.
22. Talbot J, Tarjus G, Van Tassel PR, Viot P. Colloid Surface A. 2000; 165:287–324.
23. Tie YR, Ngankam AP, Van Tassel PR. Langmuir. 2004; 20:10599–10603. [PubMed: 15544390]
24. Clark AJ, Kotlicki A, Haynes CA, Whitehead LA. Langmuir. 2007; 23:5591–5600. [PubMed: 17425343]
25. Fernsler J. Langmuir. 2011; 27:148–157. [PubMed: 21126036]
26. Schwalbe H, Grimshaw SB, Spencer A, Buck M, Boyd J, Dobson CM, Redfield C, Smith L. J. Protein Sci. 2001; 10:677–688.

27. Smith LJ, Sutcliffe MJ, Redfield C, Dobson CM. J. Mol. Biol. 1993; 229:930–944. [PubMed: 8445657]
28. McCammon JA, Gelin BR, Karplus M, Wolynes PG. Nature. 1976; 262:325–326. [PubMed: 958384]
29. Fullerton GD, Ord VA, Cameron IL. Biochim. Biophys. Acta. 1986; 869:230–246. [PubMed: 3947638]
30. Svergun DI, Richard S, Koch MHJ, Sayers Z, Kuprin S, Zaccai G. P. Natl. Acad. Sci. USA. 1998; 95:2267–2272.
31. Merzel F, Smith JC. P. Natl. Acad. Sci. USA. 2002; 99:5378–5383.
32. Hess B, Kutzner C, van der Spoel D, Lindahl E. J. Chem. Theory Comput. 2008; 4:435–447.
33. Hlady V, Buijs J. Curr. Opin. Biotechnol. 2002; 7:72–77. [PubMed: 8791316]
34. Kubiak K, Mulheran PA. J. Phys. Chem. B. 2009; 113:12189–12200. [PubMed: 19518099]
35. Lounnas V, Pettitt BM, Phillips GN. Biophys. J. 1994; 66:601–614. [PubMed: 8011893]
36. Makarov V, Pettitt BM, Feig M. Accounts Chem. Res. 2002; 35:376–384.
37. Rudnicki WR, Pettitt BM. Biopolymers. 1997; 41:107–119. [PubMed: 8986123]
38. Blake CCF, Koenig DF, Mair GA, North ACT, Phillips DC, Sarma VR. Nature. 1965; 206:757–761. [PubMed: 5891407]
39. Kepka AG, Grossweiner LI. Photochem. Photobiol. 1973; 18:49–61. [PubMed: 4795549]
40. Sethuraman A, Vedantham G, Imoto T, Przybycien T, Belfort G. Proteins. 2004; 56:669–678. [PubMed: 15281120]
41. Kabsch W, Sander C. Biopolymers. 1983; 22:2577–2637. [PubMed: 6667333]
42. Matagne A, Radford SE, Dobson CM. J. Mol. Biol. 1997; 267:1068–1074. [PubMed: 9150396]
43. Miranker A, Robinson CV, Radford SE, Aplin RT, Dobson CM. Science. 1993; 262:896–900. [PubMed: 8235611]
44. Radford SE, Dobson CM, Evans PA. Nature. 1992; 358:302–307. [PubMed: 1641003]
45. Raffaini G, Ganazzoli F. Langmuir. 2010; 26:5679–5689. [PubMed: 20041676]
46. Cadman AD, Fleming R, Guy RH. Biophys. J. 1981; 37:569–574. [PubMed: 7074186]
47. Shaw DE, Maragakis P, Lindorff-Larsen K, Piana S, Dror RO, Eastwood MP, Bank JA, Jumper JM, Salmon JK, Shan Y, Wriggers W. Science. 2010; 330:341–346. [PubMed: 20947758]

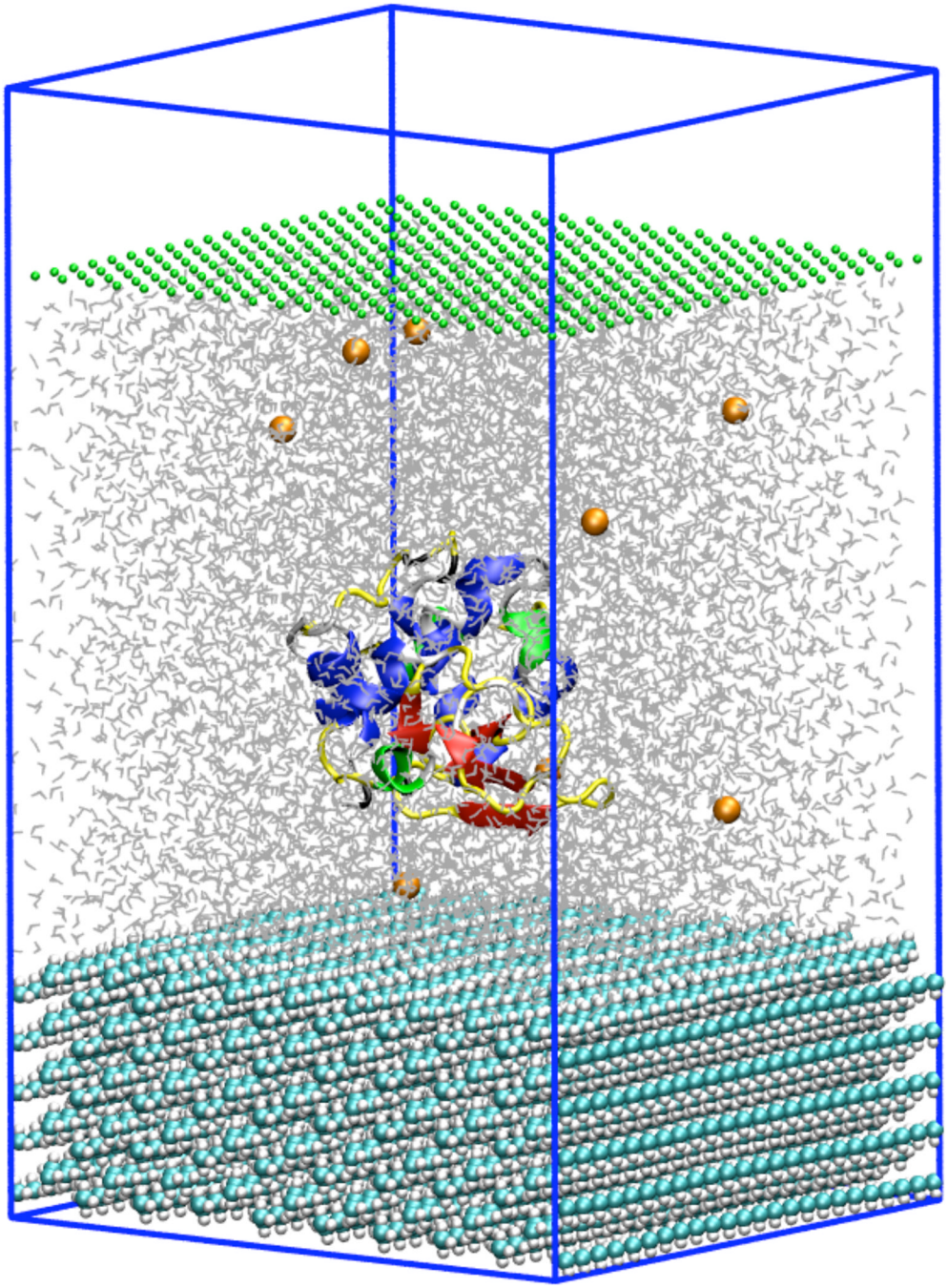

**Figure 1.**
Snapshot of the initial configuration of a lysozyme molecule on a PE (010) surface in an aqueous environment with counter ions ($Cl^-$). The PE surface atoms are shown in cyan (carbon) and white (hydrogen); counter ions are in orange, water molecules are in grey and the artificial atoms in the capped layers are in green. The ethylene chains are aligned in the direction of *y*-axis. *z*-direction is normal to the PE surface.

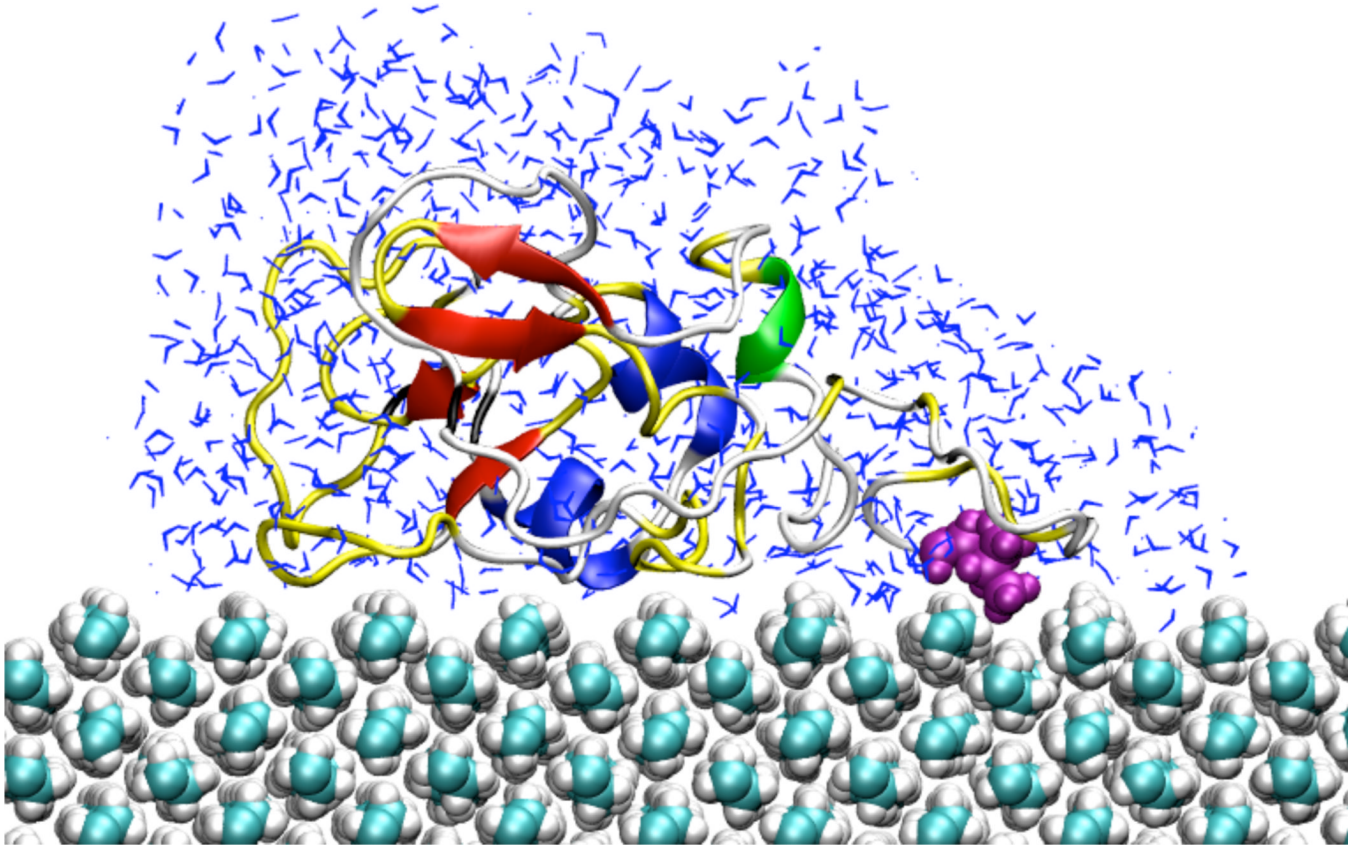

**Figure 2.**
Protein, surface and some of the solvating water molecules at the final stages of simulation, i.e. at t=300 ns. The last residue, containing the C terminal is displayed in magenta.

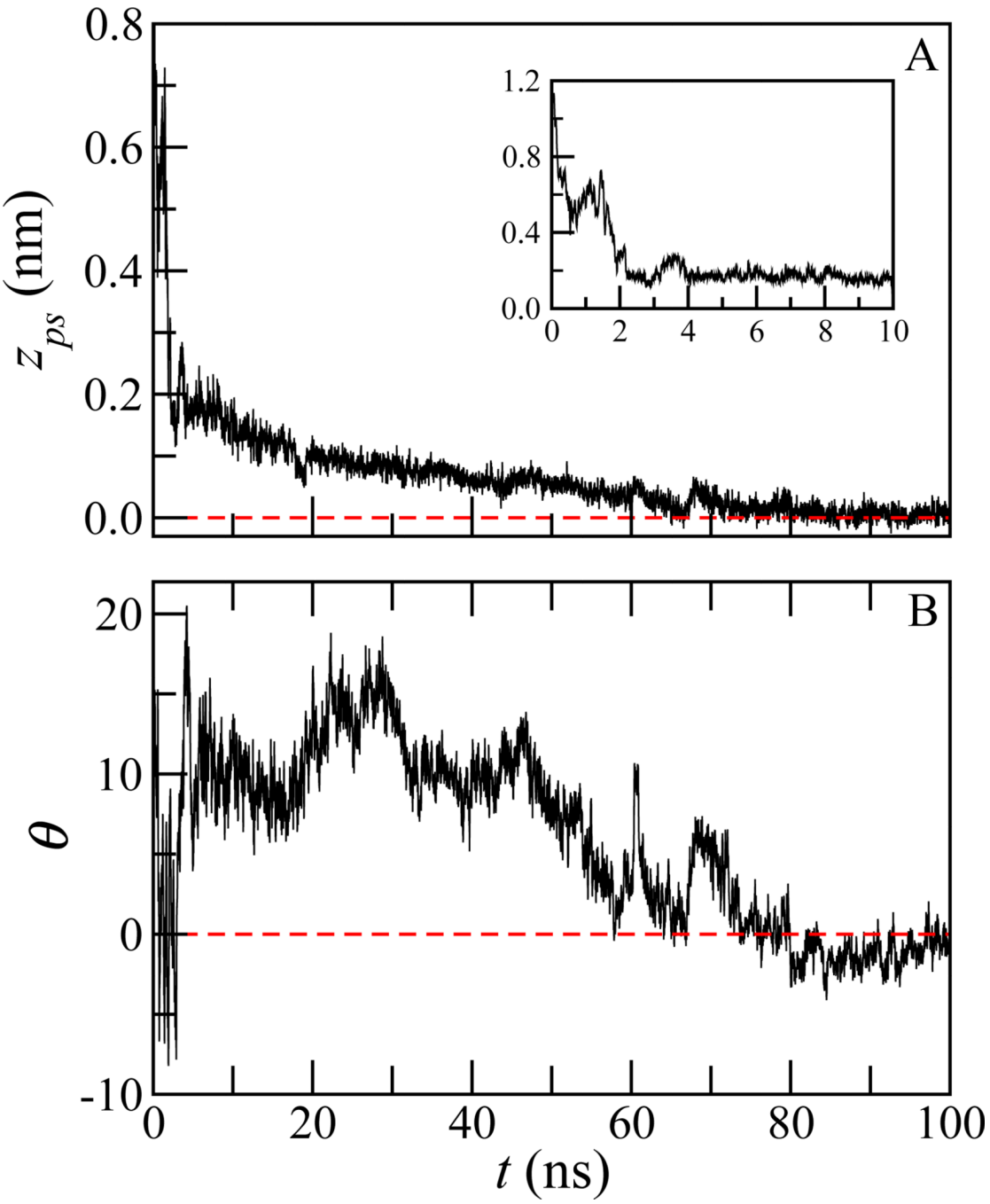


**Figure 3.**

A) The distance of closest approach between the protein and the surface as a function of time. The inset shows the initial part of the simulation. B) The orientation as a function of time. Both A) and B) are shown only for the first 100 ns.

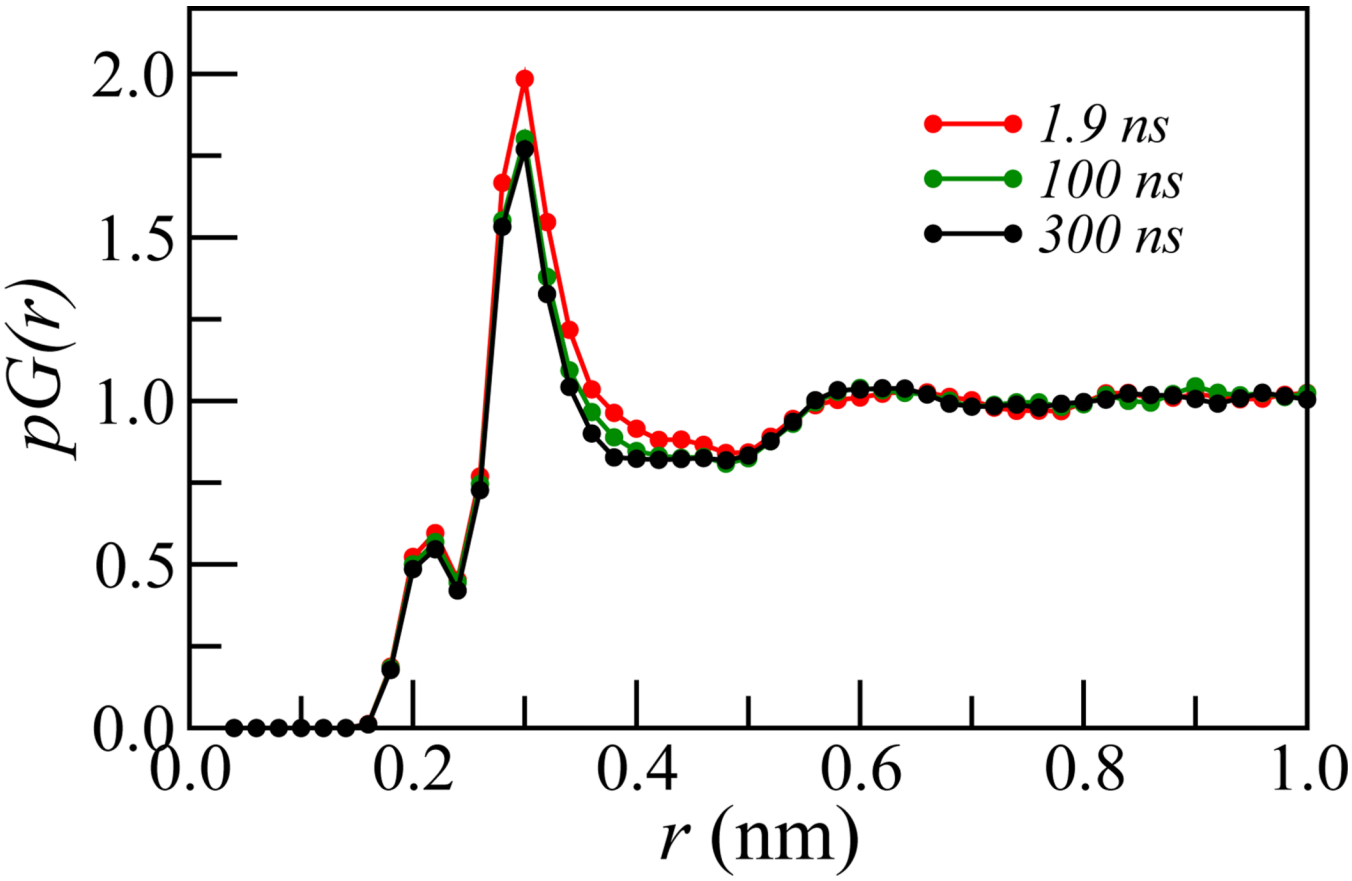


**Figure 4.**
Proximal radial distribution function for the oxygen atoms of the water from the lysozyme at three different times during the simulation.

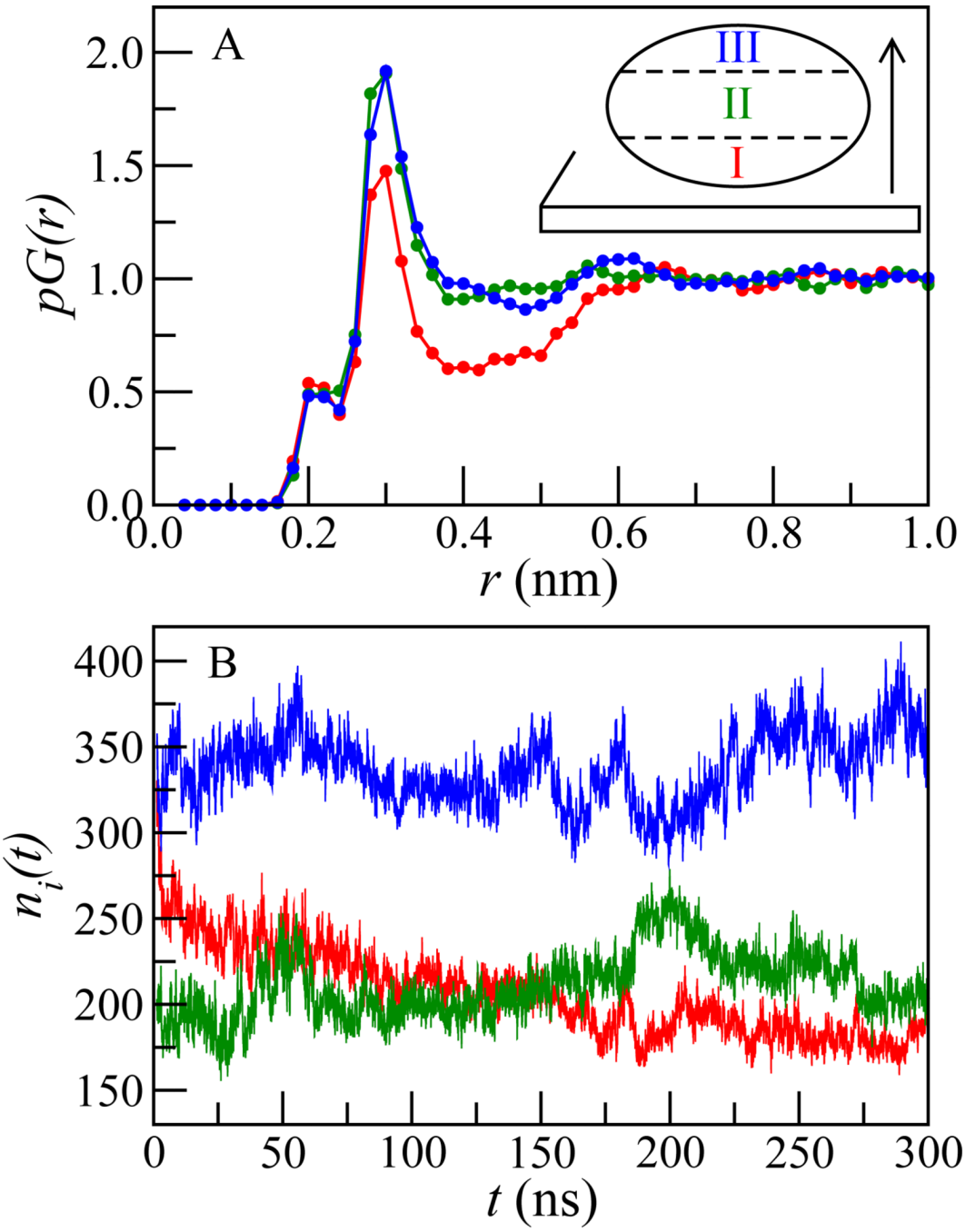


**Figure 5.**

A) Proximal radial distribution function for different regions of the protein at *t*=300 ns. B) Number of water molecules within the first hydration shell of the three different regions as a function of time.

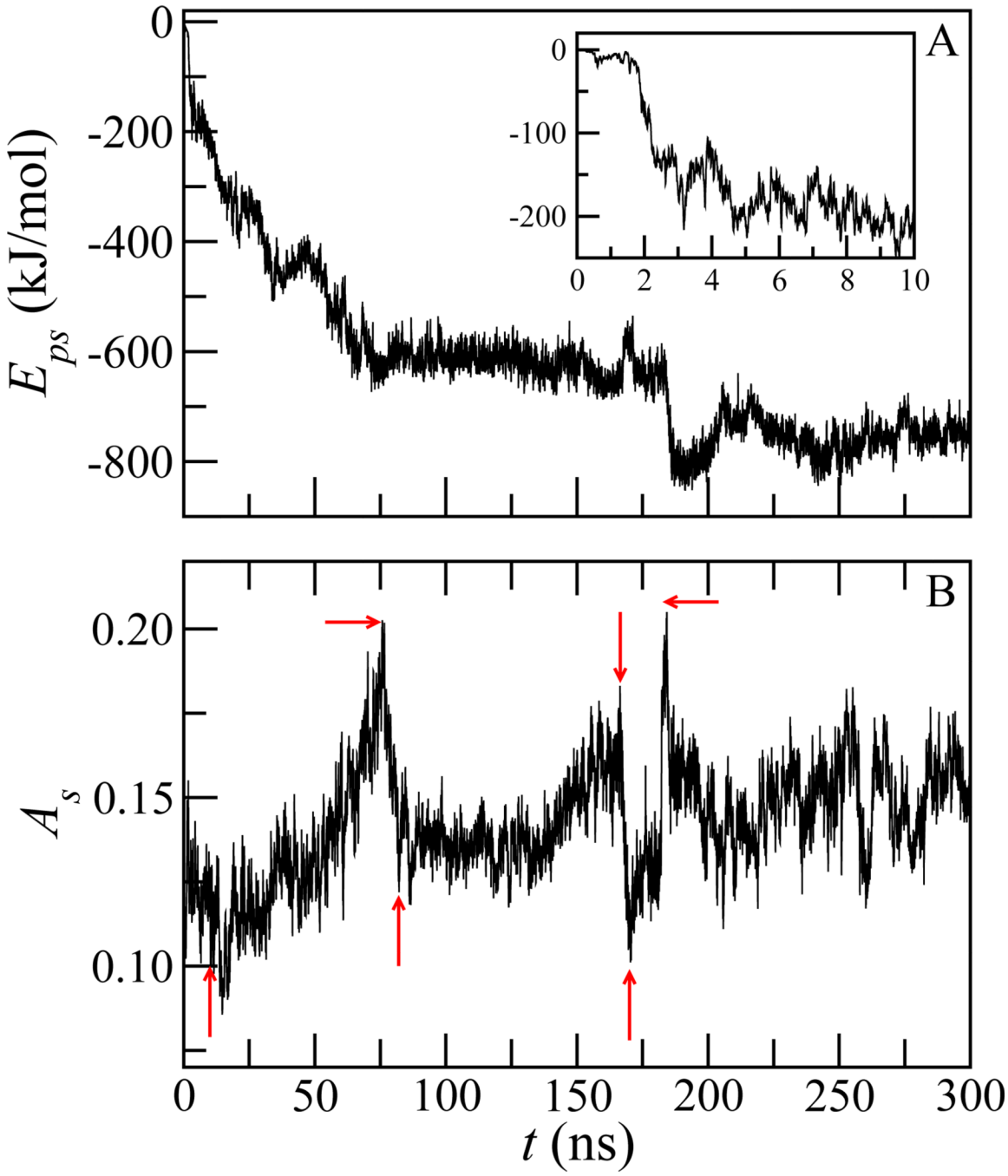


**Figure 6.**
A) Total interaction energy between the protein and the surface as a function of time. The inset shows the initial approach to the surface. B) Proteins asphericity as a function of time. The arrows indicate the times of significant changes for further analysis. From left to right, these times are 10 ns, 76 ns, 82 ns, 166 ns, 170 ns and 183 ns, respectively.

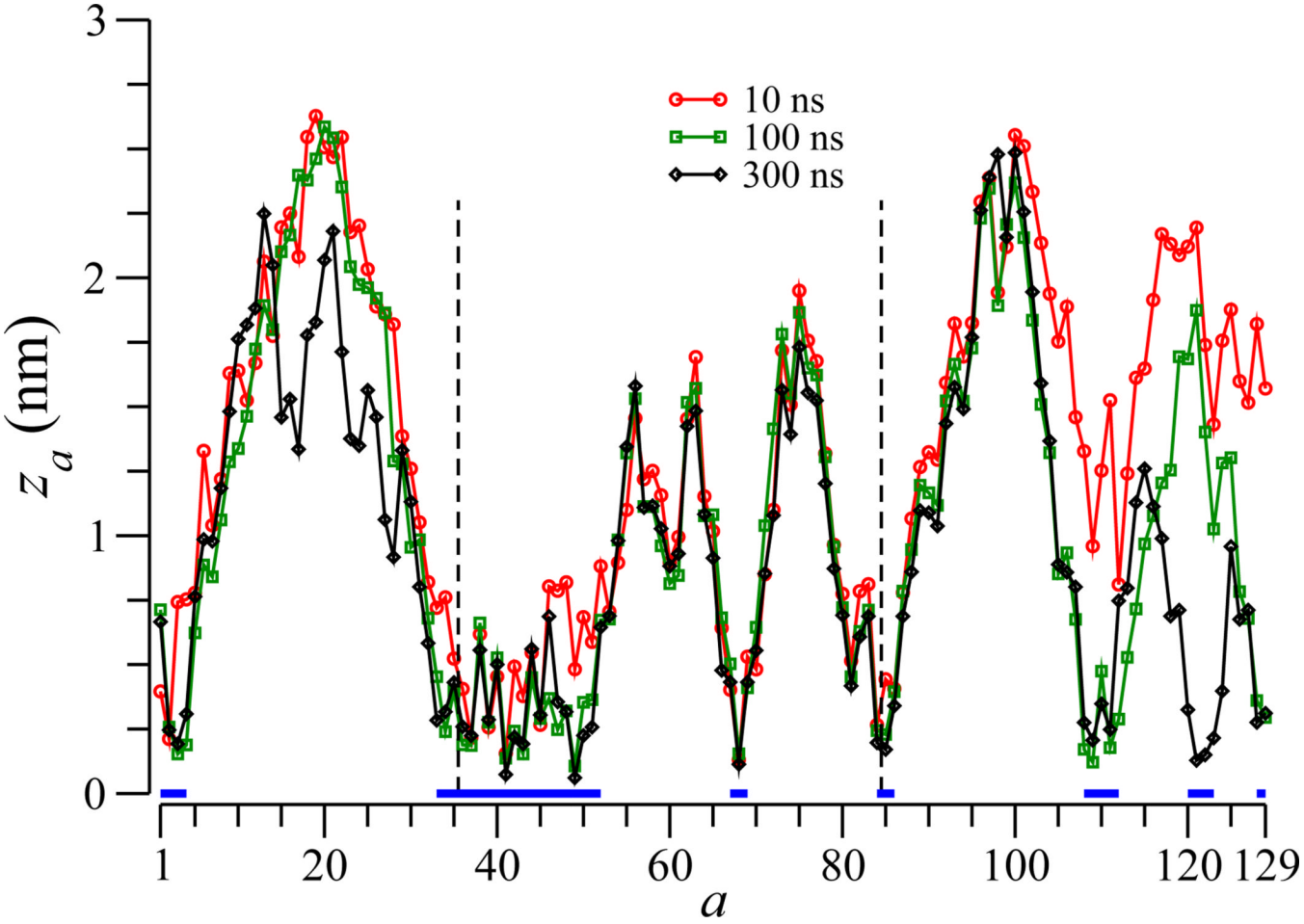


**Figure 7.**
Distance of residue's COM to the surface (The value of 0 in distance represents the position of top surface atoms) at three different times: 10 ns (red), 100 ns (green), and 300 ns (black). Residues of the lysozyme are divided into three sections: the first part of α-domain (1–35), the β-domain (36–84), and the second part of α-domain (85–129). Adsorption sites are indicated by the blue horizontal lines and are labeled 1 to 7 from left to right.

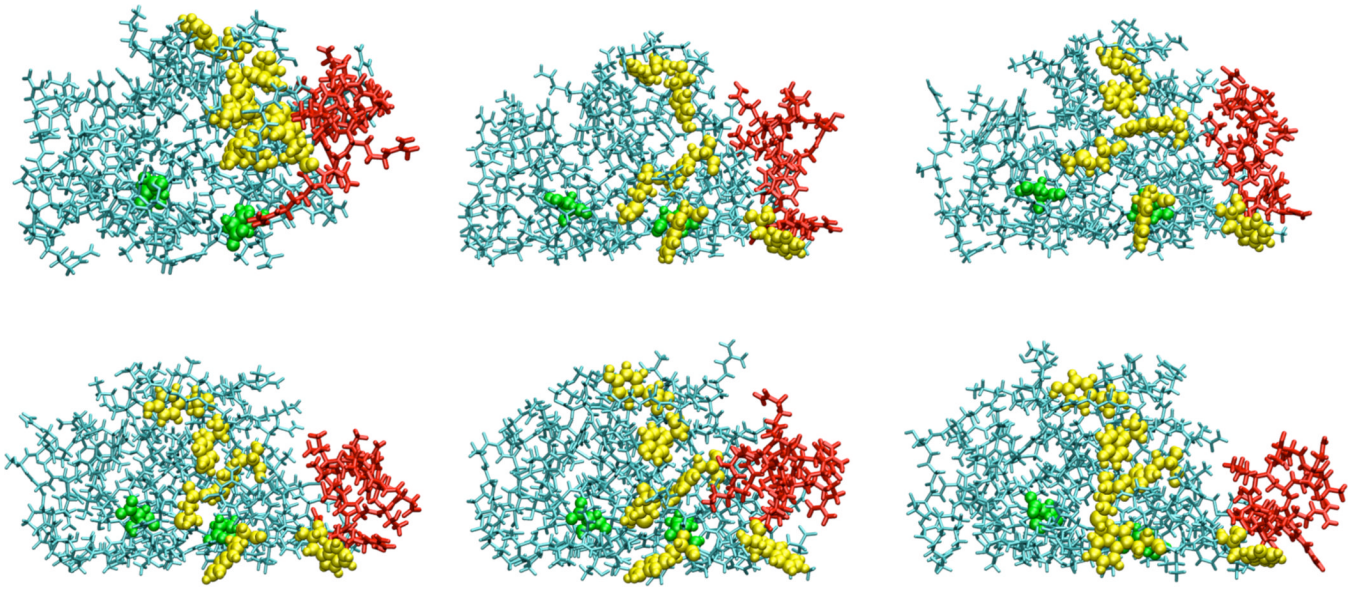

**Figure 8.**
Snapshots corresponding to the times indicated in Figure 6B: 10 ns, 76 ns, 82 ns, 166 ns, 170 ns, 183 ns. The colors of the snapshots represent, Yellow: the residues of hydrophobic pockets (Tyr20, Tyr23, Trp28, Met105, Trp108 and Trp111); Red: residues (112–125) in α-domain; Green: residues (Glu35,Asp52) active sites; Cyan: all the other protein atoms.

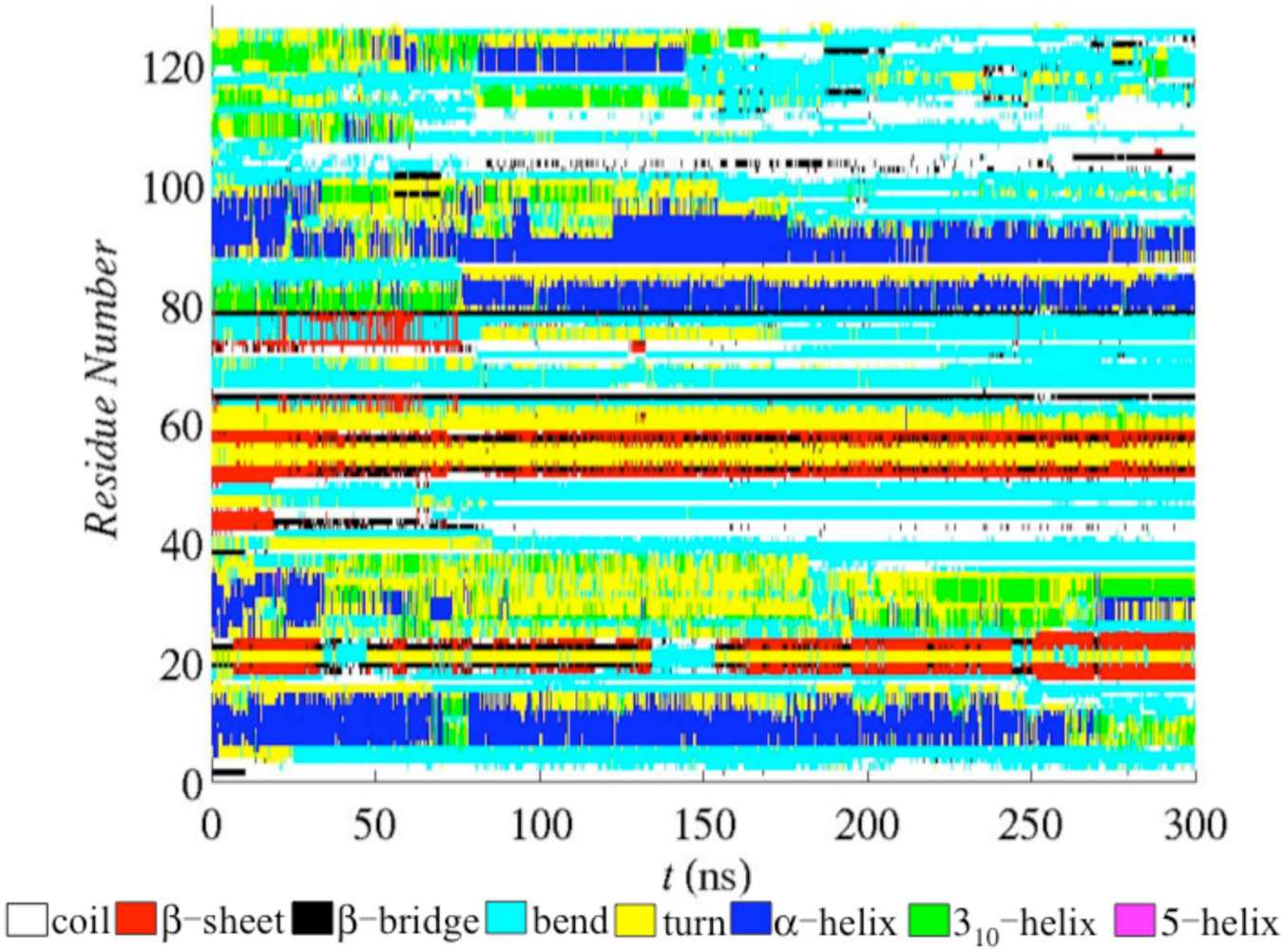


**Figure 9.**
Time evolution of the secondary structure of lysozyme.